New Phytologist

Research

Elongation factor 1 is a component of the *Arabidopsis* RNA polymerase II elongation complex and associates with a subset of transcribed genes

Hanna Markusch[1], Philipp Michl-Holzinger[1], Simon Obermeyer[1], Claudia Thorbecke[1], Astrid Bruckmann[2], Sabrina Babl[3], Gernot Längst[3], Akihisa Osakabe[4], Frédéric Berger[4] and Klaus D. Grasser[1]

[1]Cell Biology & Plant Biochemistry, Centre for Biochemistry, University of Regensburg, Universitätsstr. 31, D-93053 Regensburg, Germany; [2]Institute for Biochemistry I, Centre for Biochemistry, University of Regensburg, Universitätsstr. 31, D-93053 Regensburg, Germany; [3]Institute for Biochemistry III, Centre for Biochemistry, University of Regensburg, Universitätsstr. 31, D-93053 Regensburg, Germany; [4]Gregor Mendel Institute (GMI), Austrian Academy of Sciences, Vienna BioCenter (VBC), Dr. Bohr-Gasse 3, 1030 Vienna, Austria

Author for correspondence:
Klaus D. Grasser
Email: klaus.grasser@ur.de

Received: *20 July 2022*
Accepted: *24 December 2022*

New Phytologist (2023) **238:** 113–124
doi: 10.1111/nph.18724

Key words: *Arabidopsis thaliana*, chromatin, gene activity, mRNA synthesis, RNA polymerase II, transcript elongation.

Summary

- Elongation factors modulate the efficiency of mRNA synthesis by RNA polymerase II (RNAPII) in the context of chromatin, thus contributing to implement proper gene expression programmes. The zinc-finger protein elongation factor 1 (ELF1) is a conserved transcript elongation factor (TEF), whose molecular function so far has not been studied in plants.
- Using biochemical approaches, we examined the interaction of *Arabidopsis* ELF1 with DNA and histones *in vitro* and with the RNAPII elongation complex *in vivo*. In addition, cytological assays demonstrated the nuclear localisation of the protein, and by means of double-mutant analyses, interplay with genes encoding other elongation factors was explored. The genome-wide distribution of ELF1 was addressed by chromatin immunoprecipitation.
- ELF1 isolated from *Arabidopsis* cells robustly copurified with RNAPII and various other elongation factors including SPT4-SPT5, SPT6, IWS1, FACT and PAF1C. Analysis of a CRISPR-Cas9-mediated gene editing mutant of *ELF1* revealed distinct genetic interactions with mutants deficient in other elongation factors. Moreover, ELF1 associated with genomic regions actively transcribed by RNAPII. However, ELF1 occupied only *c.* 33% of the RNAPII transcribed loci with preference for inducible rather than constitutively expressed genes.
- Collectively, these results establish that *Arabidopsis* ELF1 shares several characteristic attributes with RNAPII TEFs.

Introduction

Production of mRNAs by RNA polymerase II (RNAPII) is characterised by several consecutive steps including promoter recruitment, initiation, elongation and termination. Over the last years, it became clear that in addition to initiation, the elongation stage is dynamic and heavily regulated. Consequently, a range of transcript elongation factors (TEFs) was identified that facilitate efficient mRNA synthesis from nucleosomal templates (Sims *et al.*, 2004; Kwak & Lis, 2013; Chen *et al.*, 2018; Osman & Cramer, 2020). During ongoing transcription, TEFs serve diverse functions assisting the progression of RNAPII through repressive chromatin. Accordingly, some TEFs modulate the catalytic properties and processivity of RNAPII, while others act as histone chaperones or chromatin remodelling factors assisting progression of RNAPII through nucleosomes. Another group of TEFs modifies transcribed chromatin through deposition/erasure of transcription-related histone marks such as mono-ubiquitination or a variety of methylations and acetylations (Sims *et al.*, 2004; Kwak & Lis, 2013; Chen *et al.*, 2018; Osman & Cramer, 2020).

A specific example of the heterogenous family of TEFs is elongation factor 1 (ELF1) that originally was identified in a yeast genetic screen by virtue of the synthetic lethality of the *elf1Δ* mutant in combination with mutations in genes encoding other known TEFs (Prather *et al.*, 2005). ELF1 is a small zinc-finger protein that is conserved in eukaryotes and some archaea. It was found to interact functionally with various other TEFs including SPT4-SPT5, TFIIS, FACT and PAF1C, and it preferentially localises to genomic regions that are actively transcribed by RNAPII (Prather *et al.*, 2005; Mayer *et al.*, 2010; Rossi *et al.*, 2021). Based on its steady association with the yeast RNAPII elongation complex during *in vitro* transcription, ELF1 was designated as core elongation factor (Joo *et al.*, 2019). Using a combination of cryo-EM and X-ray crystallography, it recently could be clarified that ELF1 directly interacts with RNAPII at the DNA entry tunnel of downstream DNA (Ehara *et al.*, 2017). Further *in vitro* studies demonstrated that ELF1 (particularly in cooperation with

SPT4-SPT5) promoted progression of RNAPII through the nucleosomal barrier during transcriptional elongation (Ehara *et al.*, 2019). The human orthologue ELOF1 can facilitate RNAPII ubiquitination and is also involved in transcription-coupled DNA repair (van der Weegen *et al.*, 2021). In archaea, ELF1 was identified as part of the elongation complex, promoting productive transcript elongation (Blombach *et al.*, 2021).

In plants, various TEFs have been identified and studies primarily in *Arabidopsis* have demonstrated that by establishing proper gene expression programmes they modulate growth and development (van Lijsebettens & Grasser, 2014). A number of TEFs associate with elongating *Arabidopsis* RNAPII to form the active elongation complex that also integrates the cooperation with cotranscriptional processes (Antosz *et al.*, 2017). *Arabidopsis* factors modulating RNAPII properties during elongation (e.g. TFIIS and SPT4-SPT5) influence hormone signalling, stress response and germination (Grasser *et al.*, 2009; Dürr *et al.*, 2014; Antosz *et al.*, 2020; Szádeczky-Kardoss *et al.*, 2022), while transcription-related histone chaperones (e.g. SPT6L, FACT) are required for normal embryo development, seedling establishment and developmental transitions (Lolas *et al.*, 2010; Gu *et al.*, 2012; Chen *et al.*, 2019). Various factors that affect the deposition of histone marks over transcribed regions (e.g. PAF1-C, HUB1/2 and SDG proteins) have profound effects on many aspects of plant growth and development (He *et al.*, 2004; Oh *et al.*, 2004; Fleury *et al.*, 2007; Xu *et al.*, 2008; Berr *et al.*, 2010; Fiorucci *et al.*, 2019).

A putative orthologue of yeast ELF1 (and mammalian ELOF1) is encoded in *Arabidopsis* (and other plant genomes), but so far, its molecular function has not been studied. Therefore, we have characterised ELF1 from *Arabidopsis* that proved to be a nuclear protein associated with elongating RNAPII. ELF1 interacts *in vitro* with DNA and histones, and it localises to genomic regions that are actively transcribed by RNAPII. Examination of respective mutant plants demonstrated genetic interactions between *ELF1* and genes encoding other known TEFs. Taken together, these findings illustrate that *Arabidopsis* ELF1 is the counterpart of yeast ELF1 (and mammalian ELOF1) acting in RNAPII transcriptional elongation.

Materials and Methods

Recombinant protein production

Using pET24 expression vectors (Supporting Information Table S1), ELF1 proteins fused to a GB1/6xHis-tag were expressed in *Escherichia coli* and bound to Ni-NTA-agarose (Qiagen). Full-length and truncated ELF1 proteins were eluted by cleavage with the HRV 3C protease (Sigma), removing the GB1/6xHis-tag. Subsequently, recombinant proteins were purified by ion-exchange FPLC using a Resource S Column (GE Healthcare, Freiburg, Germany) and proteins were eluted with a linear gradient 0–1 M NaCl in buffer D (10 mM sodium phosphate, pH 7.0, 1 mM EDTA, 1 mM dithiothreitol, 0.5 mM PMSF) as described previously (Grasser *et al.*, 1996). Recombinant *Arabidopsis* histones H2A-H2B were prepared as described previously (Osakabe *et al.*, 2018). Purified proteins were characterised by SDS-PAGE and mass spectrometry.

Electrophoretic mobility shift assays

DNA-binding of recombinant ELF1 proteins was examined by electrophoretic mobility shift assays (EMSAs) with Cy5-labelled DNA oligonucleotides (Table S2) that were either annealed to linear double strands or to four-way junctions (4wjs). Binding reactions were analysed in 6% polyacrylamide 1× TBE gels and DNA was visualised using a ChemiDoc MP Imaging System (Bio-Rad). Interactions with nucleosomes and the corresponding nucleosomal DNA were examined as described previously (Pfab *et al.*, 2018).

Intramolecular crosslinking with EDC

Recombinant ELF1 proteins were incubated for different periods in buffer D (10 mM sodium phosphate, pH 7.0, 1 mM EDTA, 1 mM dithiothreitol, 0.5 mM PMSF) with a final concentration of 20 mM 1-ethyl-3-(3-dimethylaminopropyl)carbodiimide (EDC; Sigma) from a freshly prepared stock as described previously (Thomsen *et al.*, 2004). Subsequently, samples were analysed by SDS-PAGE and Coomassie staining.

GST pull-down assays

Protein interaction assays were essentially performed as described previously (Michl-Holzinger *et al.*, 2022), with recombinant ELF1 proteins fused to glutathione S transferase (GST) mixed with equimolar amounts of recombinant *Arabidopsis* H2A-H2B or with bovine cytochrome C (CytC; Sigma Aldrich) in GST buffer (0.2–0.35 M NaCl, 25 mM HEPES pH 7.6, 0.05% (v/v) NP40, 5 mM DTT, 10% (v/v) glycerol, 2 mM $MgCl_2$). Following incubation (30 min at 30°C), glutathione-sepharose beads were added and the samples were incubated for 3 h on a rotating wheel at 4°C. Beads were washed three times in GST buffer before bound proteins were eluted by boiling in protein loading buffer and analysed by SDS-PAGE.

Affinity purification and characterisation of GS-tagged ELF1 from *Arabidopsis* cells

Arabidopsis suspension-cultured PSB-D cells were maintained and transformed as described previously (van Leene *et al.*, 2015). Protein isolation, purification of GS-tagged (protein G and streptavidin-binding peptide-tagged) ELF1 using IgG-coupled magnetic beads, mass spectrometry and data analyses including removal of experimental background were performed as described previously (Dürr *et al.*, 2014; Antosz *et al.*, 2017).

Plant material

Seeds of *Arabidopsis thaliana* (L.) Heynh. (ecotype Col-0) were stratified in darkness for 48 h at 4°C, and plants were grown at 21°C on soil in a phytochamber or on MS medium in plant

incubators (PolyKlima, Freising, Germany) under long-day conditions (Antosz *et al.*, 2017; Michl-Holzinger *et al.*, 2022). Col-0 plants expressing eGFP-NLS were described previously (Pfab *et al.*, 2018).

CRISPR-Cas9-mediated gene editing

CRISPR-Cas9 gene-edited plant lines were generated in the Col-0 background utilising egg cell-specific promoter-controlled Cas9 vector systems (Wang *et al.*, 2015). A specific sgRNA sequence was selected using the tool CRISPR-P 2.0 (Liu *et al.*, 2017). For the *ELF1* sgRNA, complementary oligonucleotides (Table S2) were annealed and inserted into pHEE401E (Wang *et al.*, 2015) via Golden Gate assembly using BsaI restriction sites, generating the transformation vector (Table S1) that was introduced into *Arabidopsis* Col-0 by *Agrobacterium*-mediated transformation as described previously (Lolas *et al.*, 2010; Dürr *et al.*, 2014). For genotyping of CRISPR-Cas9 mutants, genomic DNA was isolated from leaves and used as template for PCR with primers specified in Table S2, before the amplified fragments were analysed by DNA sequencing.

Generation and analysis of *Arabidopsis* double mutants

Arabidopsis double-mutant plants (all ecotype Col-0) were generated by genetic crossing, as described previously (Lolas *et al.*, 2010), of gene-edited *elf1-1* and *tfIIs-1* (SALK_056755; Grasser *et al.*, 2009), *ssrp1-2* (SALK_001283; Lolas *et al.*, 2010) or *iws1-1* (SALK_056238; Li *et al.*, 2010). Complementation analyses were performed with double-mutant plants crossed with *elf1-1*^{C1} (to be described later). Obtained plants were verified by PCR-based genotyping (using primers listed in Table S2) and DNA sequencing. Plant phenotypes were generally analysed and documented as described previously (Lolas *et al.*, 2010; Dürr *et al.*, 2014), while leaf serration was determined according to Bilsborough *et al.* (2011) and leaf angles according to Hopkins *et al.* (2008).

Confocal laser scanning microscopy

Confocal laser scanning microscopy (CLSM) was performed using a Zeiss LSM 980 Airyscan2, equipped with a 10× NA 0.3, a 20× NA 0.3, a 40× Oil 1.3 or 63× Oil NA 1.3 objective. eGFP and propidium iodide (PI) were excited using a VIS Laser at 488 and 561 nm, respectively. The emission of eGFP was detected at 500–550 nm, while the emission of PI was detected at 570–620 nm.

ChIP sequencing

Chromatin immunoprecipitation (ChIP) was essentially performed as described previously (Antosz *et al.*, 2020; Michl-Holzinger *et al.*, 2022). *Arabidopsis* plants (14 d after stratification, 14-DAS *in vitro* grown) were crosslinked with formaldehyde and used for isolation of nuclei, before chromatin was sheared using a Bioruptor Pico device (Diagenode, Seraing, Belgium). Immunoprecipitation was performed using antibodies directed against GFP (ab290; Abcam, Berlin, Germany) and S2P-modified (Ser2-phosphorylated heptapeptides of the carboxy-terminal domain of NRPB1) RNAPII (ab5095; Abcam). For ChIP sequencing (ChIP-Seq), libraries were generated using NEBNext Ultra II DNA Library Prep Kit for Illumina (NEB, Frankfurt, Germany) and the final libraries (four and three replicates each for ELF1-eGFP and S2P-RNAPII, respectively) were sequenced by the Genomics Core Facility at the University of Regensburg (http://www.kfb-regensburg.de/) using NextSeq 2000 (Illumina, San Diego, CA, USA). Reads were aligned to the TAIR10 genome (https://www.arabidopsis.org/) using Bowtie2 (Langmead & Salzberg, 2012), and coverage tracks were calculated with deepTools 'bamCoverage' (Table S3). Downstream analysis was mainly performed using the deepTools2 suite (v.3.5.0; Ramírez *et al.*, 2016), and quality control was performed at several steps using FastQC (Ewels *et al.*, 2016). In case of RNAPII-S2P, 12.3–18.8 M reads and for ELF1-eGFP 12.1–23.1 M reads mapped against the TAIR10 genome. Genomic regions with aberrant coverage or low sequence complexity were filtered out, as described previously (Quadrana *et al.*, 2016). After confirming high pairwise correlations, the biological replicates were merged and CPM normalised. Macs3 callpeak was used to call peaks over input as control. Gene Ontology (GO)-term enrichments have been performed with Shiny GO (Ge *et al.*, 2020). Expression levels of genes (divided into genes > 28 and < 0.01 TPMs) were deduced from RNA sequencing data (Michl-Holzinger *et al.*, 2022) of *in vitro* grown 6-DAS Col-0 plants under standard conditions, which was performed in three replicates.

Results

ELF1 interacts with DNA, histones and nucleosomes

To identify putative *Arabidopsis* orthologues of yeast ELF1 and human ELOF1, we searched the *Arabidopsis* database (https://www.arabidopsis.org/) with the Blastp program using these amino acid sequences as a query. The search revealed a single clear hit (AGI locus At5g46030) encoding a 120-aa protein (13.9 kDa) rich in charged amino acid residues, in the following termed *Arabidopsis* ELF1. Alignments revealed that *Arabidopsis* ELF1 shares 32.9%, 33.1%, 59.2% and 81.0% amino acid sequence identity with its orthologues from *Saccharomyces cerevisiae*, *Homo sapiens*, *Oryza sativa* and *Brassica napus*, respectively (Fig. S1). It is comprised of a basic N-terminal region, the central Zn-finger region, the RNAPII-binding region and an acidic C-terminal region. A major part of the ELF1 sequences is considerably conserved, but the acidic region is lacking in metazoan sequences and is quite heterogeneous in plant sequences (Fig. S1). For some reason, the acidic region appears to be more extended in ELF1 sequences of *Brassicacea*.

Recombinant ELF1 proteins were expressed in *E. coli* and purified to examine their molecular interactions. In addition to full-length ELF1, truncated versions lacking the basic N-terminal region (ELF1ΔN) or the acidic C-terminal region (ELF1ΔC) were produced (Fig. 1a,b). DNA binding of the ELF1 proteins was analysed using EMSAs with four-way junction (4wj) DNA

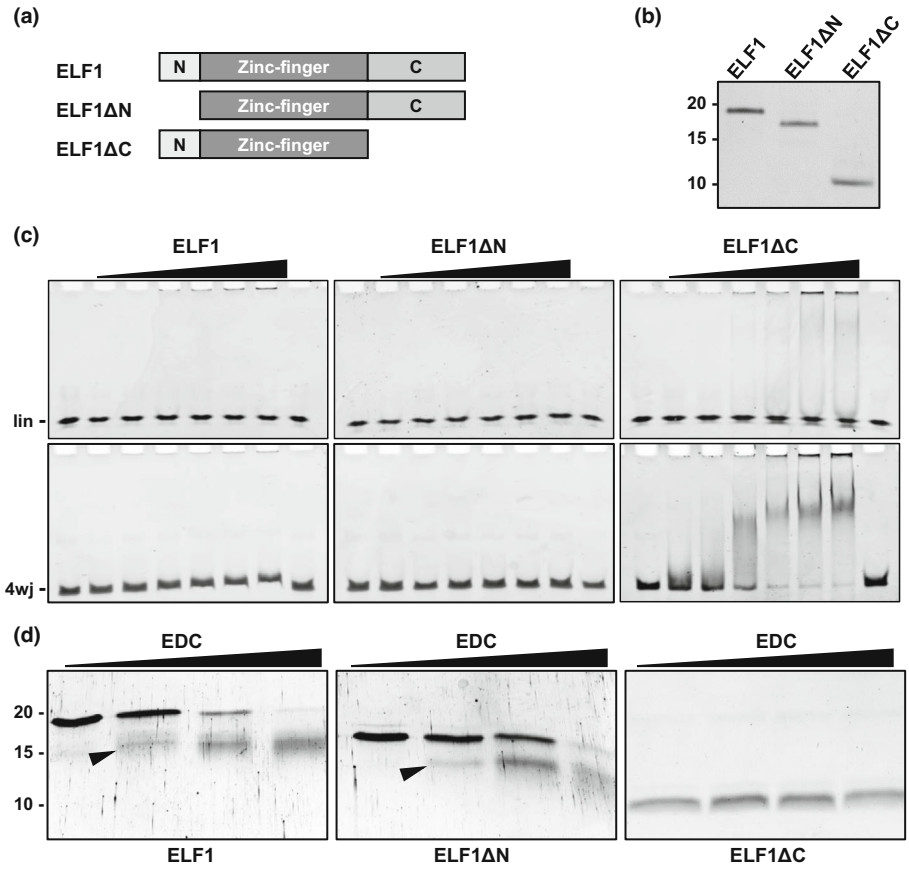

Fig. 1 DNA interactions of ELF1 are inhibited by the acidic C-terminal region.
(a) Schematic illustration of ELF1 and truncated versions. N, basic N-terminal region; zinc-finger region; C, acidic C-terminal region. (b) Purified recombinant ELF1 proteins analysed by SDS-PAGE and stained with Coomassie. (c) Electrophoretic mobility shift assays of increasing concentrations of the indicated ELF1 proteins (0, 1, 2.5, 5, 7.5, 10, 15, 0 μM, from left to right) and linear (lin, upper) or four-way junction DNA (lower). (d) The indicated ELF1 proteins were chemically crosslinked for increasing periods (0, 5, 10 and 20 min) with EDC (1-ethyl-3-(3-dimethylaminopropyl) carbodiimide), before proteins were separated on tricine polyacrylamide gels and stained with Coomassie. Intramolecular crosslinking is evident with ELF1 and ELF1ΔN from the reaction time-dependent appearance of an additional, faster migrating protein band (arrowhead).

or the corresponding linear double-stranded DNA. Four-way junction DNA was chosen, since it resembles some features of a nucleosome, as two juxtaposed DNA duplexes of the junction in a way mimic the entry/exit point of the nucleosomal DNA (Zlatanova & van Holde, 1998).

Increasing concentrations of the ELF1 proteins were incubated with the DNA, and the formation of protein/DNA complexes was examined by electrophoresis. Binding of ELF1 was detectable only with the 4wj DNA, resulting (relative to the DNA in absence of protein) in slightly reduced migration of the DNA band with increasing protein input (Fig. 1c, left). No DNA interaction was traceable with ELF1ΔN (Fig. 1c, middle), whereas marked binding of ELF1ΔC to both types of DNA was observed (Fig. 1c, right). As evident from the disappearance of the free DNA, ELF1ΔC interacted with higher affinity with the 4wj DNA than with the linear DNA, although in both cases the relatively fuzzy migration of the protein/DNA complexes suggests rather nonspecific interaction. The remarkably increased DNA interaction of ELF1ΔC likely is caused by the absence of the acidic C-terminal region that might interact intramolecularly with basic parts of the protein. Chemical crosslinking using the zero-length agent EDC (which cross-links carboxyl and amino groups) was used to address possible intramolecular interactions of the acidic C-terminal region in ELF1. Full-length and truncated versions of ELF1 were reacted with EDC for various periods and subsequently analysed by SDS-PAGE. Intramolecular crosslinking is evident with ELF1 and ELF1ΔN from the reaction time-dependent appearance of an additional, faster migrating protein band (Fig. 1d). By contrast, ELF1ΔC lacking the acidic region could not be crosslinked, suggesting that in ELF1 and ELF1ΔN, the acidic region interacts with basic parts of the protein (basic N-terminal region and/or central region), thereby reducing the affinity for DNA.

The interaction of ELF1 with histones was studied using GST pull-down assays. ELF1 and ELF1ΔC were produced as GST fusion proteins and immobilised on gluthatione-sepharose beads. Added H2A-H2B bound to GST-ELF1, but not to GST-ELF1ΔC (Fig. 2a), suggesting that the acidic C-terminal region is required for histone interaction. Similar to the histone interaction of the acidic region of SPT16 (Michl-Holzinger *et al.*, 2022), the specificity of the ELF1–histone interaction is evident from the lack of binding of H2A-H2B to unfused GST and the lack of binding of the small basic protein CytC to GST-ELF1 in the GST pull-down assay.

Using EMSAs, the interaction of ELF1 proteins with reconstituted nucleosomes (and the corresponding 147-bp DNA fragment) was examined. No interaction of ELF1 and ELF1ΔN with DNA or nucleosomes could be detected, whereas ELF1ΔC bound both to DNA and nucleosome particles (Fig. 2b). With increasing protein concentration, the migration of the nucleosome band was gradually more retarded. In conclusion, the *in vitro* interaction studies reveal that the acidic C-terminal region of ELF1 is required for the binding to histones, but it inhibits the binding of ELF1 to DNA and nucleosomes.

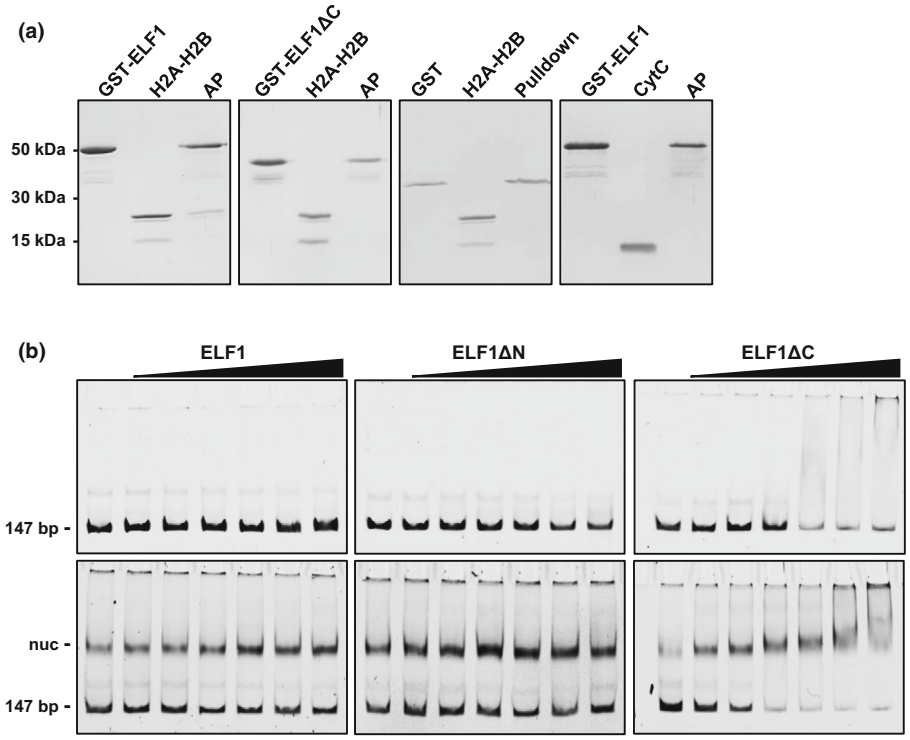

Fig. 2 ELF1 C-terminal region inhibits interactions with DNA and nucleosomes, but is required for histone binding. (a) Interaction of ELF1 with histones analysed by glutathione S transferase GST pull-down assays. The indicated GST-ELF1 fusion proteins (or unfused GST) were incubated with *Arabidopsis* H2A-H2B histones (or with cytochrome C, CytC). Binding reactions were bound to glutathione sepharose and the eluates of the affinity purification (AP) were analysed along with the input samples by SDS–PAGE and Coomassie staining. Fifty per cent of each input was loaded on an 18% SDS gel. (b) Interaction of full-length and truncated ELF1 proteins with DNA and human nucleosomes analysed by electrophoretic mobility shift assays. Increasing concentrations of the indicated ELF1 proteins (0, 1, 2.5, 5, 7.5, 10 and 15 μM, from left to right) were incubated with 147-bp DNA (upper) or a mixture of 147-bp DNA and reconstituted human mono-nucleosomes containing the 147-bp DNA (lower).

ELF1 is a component of the RNAPII transcript elongation complex

To investigate the possible association with RNAPII, ELF1 was expressed as GS-tagged fusion protein in *Arabidopsis* PSB-D suspension-cultured cells, an approach that has been used to study other RNAPII-associated proteins (Dürr *et al.*, 2014; Antosz *et al.*, 2017). ELF1-GS and interacting proteins were isolated from cell extracts by IgG affinity purification using mild conditions to preserve protein interactions. SDS–PAGE analysis revealed the enrichment of the ELF1-GS bait protein along with a number of copurifying protein bands that were not detected with the unfused GS-tag (Fig. 3a). Proteins in the eluates were identified after tryptic digestion by mass spectrometry. Strikingly, a number of RNAPII subunits were found to robustly copurify with ELF1 (Fig. 3b). In addition, several TEFs reproducibly co-eluted efficiently with ELF1 and RNAPII such as FACT (SSRP1 and SPT16), SPT4-SPT5, SPT6L, IWS1 and PAF1C (ELF7, VIP3, VIP4 and CDC73). These interactors were not identified in the control experiment with the unfused GS-tag or in comparable IgG affinity purifications of unrelated nuclear proteins (Municio *et al.*, 2021; Cheng *et al.*, 2022). This result suggests that *Arabidopsis* ELF1 along with other TEFs associates with RNAPII to form the transcript elongation complex in accord with the situation in yeast (Ehara *et al.*, 2017, 2019).

Functional inactivation of *ELF1* causes mild effects and ELF1 localises to cell nuclei

No useful T-DNA insertion mutant could be identified to study the *in planta* function of ELF1. Therefore, we generated CRISPR-Cas9-mediated gene-edited lines in the Col-0 background for that purpose. The gene editing resulted in insertion of an additional base pair within the coding sequence of exon 1 leading to a frameshift and a premature translational stop codon (Fig. S2a), hereafter referred to as *elf1-1*. The mutant plants are basically indistinguishable from the Col-0 wild-type, except that the height of mature plants is slightly increased (Fig. S2b). Likewise, the *elf1Δ* mutation caused no significant growth defect in yeast (Prather *et al.*, 2005). Following transformation of *elf1-1* plants with a complementation construct, the expression of an ELF1-eGFP fusion protein under control of the *ELF1* promoter (*c.* 4 kb upstream of transcriptional start site (TSS)) in three independent plant lines (termed *elf1-1*^{C1}, *elf1-1*^{C5} and *elf1-1*^{C6}) did not affect plant phenotype, besides reducing the increased height of *elf1-1* (Fig. S2c–e). Analysis of these plants using CLSM demonstrated that ELF1-eGFP localises to the cell nucleus (Fig. 4), as reported for human ELOF1 (van der Weegen *et al.*, 2021). In addition, the microscopic survey detected ELF1-eGFP in all analysed *Arabidopsis* leaf and root cells (Fig. 4), suggesting ubiquitous expression, consistent with publicly available *Arabidopsis* mRNA expression data regarding *ELF1* (Winter *et al.*, 2007).

Genetic interaction of *ELF1* with genes coding for other transcript elongation factors

To further elucidate the involvement of ELF1 in elongation by RNAPII, we generated double-mutant deficient in ELF1 and different previously characterised TEFs. Thus, *elf1-1* was crossed with *tfIIs-1* (Grasser *et al.*, 2009), *ssrp1-2* (Lolas *et al.*, 2010) and *iws1-1* (Li *et al.*, 2010). The obtained double-mutant plants were

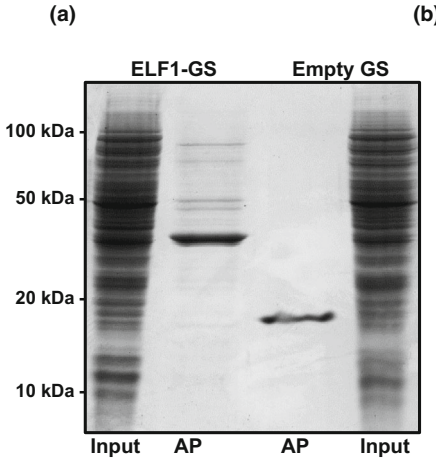

(b)

Transcript elongation related proteins copurifying with ELF1-GS

Detected	Interactor	AGI	Complex
2597.5/3	NRPB1	AT4G35800	RNAPII
2616.6/3	NRPB2	AT4G21710	RNAPII
1296.3/3	NRPB3	AT2G15430	RNAPII
421.8/3	NRPB5A	AT3G22320	RNAPII
340.2/2	NRPB7	AT5G59180	RNAPII
134.1/2	NRPB8A	AT1G54250	RNAPII
181.3/2	NRPB8B	AT3G59600	RNAPII
131.9/2	NRPB9A	AT3G16980	RNAPII
132.9/2	NRPB11	AT3G52090	RNAPII
1355.9/3	SPT16	AT4G10710	FACT
816.3/3	SSRP1	AT3G28730	FACT
87.2/2	SPT4-1	AT5G08565	SPT4-SPT5
1133.2/3	SPT5-2	AT4G08350	SPT4-SPT5
791.4/3	ELF1	AT5G46030	ELF1
1040.3/2	SPT6L	AT1G65440	SPT6
359.7/3	IWS1	AT1G32130	IWS1
230.5/3	ELF7	AT1G79730	PAF1C
343.9/3	VIP4	AT5G61150	PAF1C
92.3/3	VIP5	AT1G61040	PAF1C
332.7/3	CDC73	AT3G22590	PAF1C

Fig. 3 Affinity purification of ELF1 from *Arabidopsis* cells. (a) Total protein extract of PSB-D cells expressing ELF1-GS or the unfused GS-tag (input) was analysed by SDS-PAGE and Coomassie staining, along with the eluate of the corresponding IgG affinity purifications (AP). (b) Transcript elongation-related proteins (i.e. transcript elongation factors, RNAPII subunits) that copurified with ELF1-GS, as identified by mass spectrometry. Numbers in the left column indicate the respective average MASCOT scores and the number of times the interactor was detected in three independent affinity purifications; only proteins are listed that were detected at least twice in three experiments with significant MASCOT scores in the ELF1-GS samples, but not in controls.

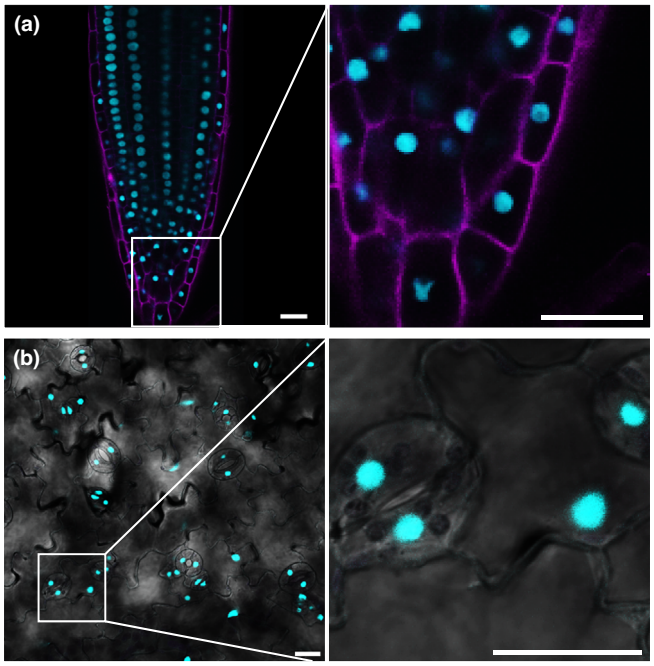

Fig. 4 ELF1 localises to nuclei of root and leaf cells. Root tips and leaves of *elf1-1* plants expressing ELF1-eGFP fusion proteins under control of the *ELF1* promoter were analysed using CLSM. (a) In root tips of 7-d after stratification (DAS) plants eGFP fluorescence is visible in cyan, while propidium iodide (PI) staining is in magenta. (b) eGFP fluorescence in the abaxial surface of leaves from 10-DAS plants (epidermal cells, guard cells). Bar, 20 μm.

phenotypically analysed to detect possible genetic interactions between *ELF1* and the genes encoding other TEFs. Regarding the first type of double mutant, both the *elf1-1* and *tfIIs-1* parental plants exhibit essentially wild-type appearance, whereas the *elf1-1 tfIIs-1* double mutant is substantially smaller (Fig. 5a–d). The reduced growth of the double mutant is efficiently complemented in *elf1-1 tfIIs1*^{C} plants by expression of ELF1-eGFP under control of the *ELF1* promoter (Fig. 5e), which is also evident from the measured fresh weight (Fig. 5v) and the rosette diameter (Fig. S3a,b) of the plant lines. Other determined phenotypic parameters differ only slightly between the different genotypes (Fig. S3a,b). Concerning the second type of double mutant, the *elf1-1 ssrp1-2* plants show striking leaf serration (leaf margin protrusions; Bilsborough *et al.*, 2011) that is greatly enhanced compared with the *ssrp1-2* parental plants and complemented in *elf1-1 ssrp1-2*^{C} plants (Fig. 5f–m,w). Rosette diameter and bolting time are minimally changed in *elf1-1 ssrp1-2* plants compared with the *ssrp1-2* single mutant (Fig. S4a,b). Regarding the third type of double mutant, when compared to the parental lines the *elf1-1 iws1-1* double mutant is very strikingly late bolting (Fig. S5a,b) and it proved sterile. In addition, the leaf angle/inclination (angle a leaf deviates from horizontal; Hopkins *et al.*, 2008) of *elf1-1 iws1-1* plants is notably more erect than that of the parental lines and this feature is complemented in *elf1-1 iws1-1*^{C} plants (Fig. 5n–u,x). Compared with the parental lines, other phenotypic parameters are only mildly affected in the double mutant (Fig. S5a,b). Together, the genetic interactions of *ELF1* with genes encoding the TEFs TFIIS, SSRP1 and IWS1 highlight a role of ELF1 in RNAPII transcript elongation.

ELF1 associates with a subset of regions actively transcribed by RNAPII

Using the above-mentioned *elf1-1* plants expressing ELF1-eGFP, ChIP-Seq analyses were performed to examine the genome-wide distribution of ELF1. To that end, ChIP was carried out with antibodies directed against eGFP, while as ChIP-Seq controls served comparable ChIP analyses with plants expressing GFP-NLS (GFP fused to a nuclear localisation signal) and ChIP input samples. Analysis of the ChIP-Seq data revealed that biological replicates yielded robust results that group together and are

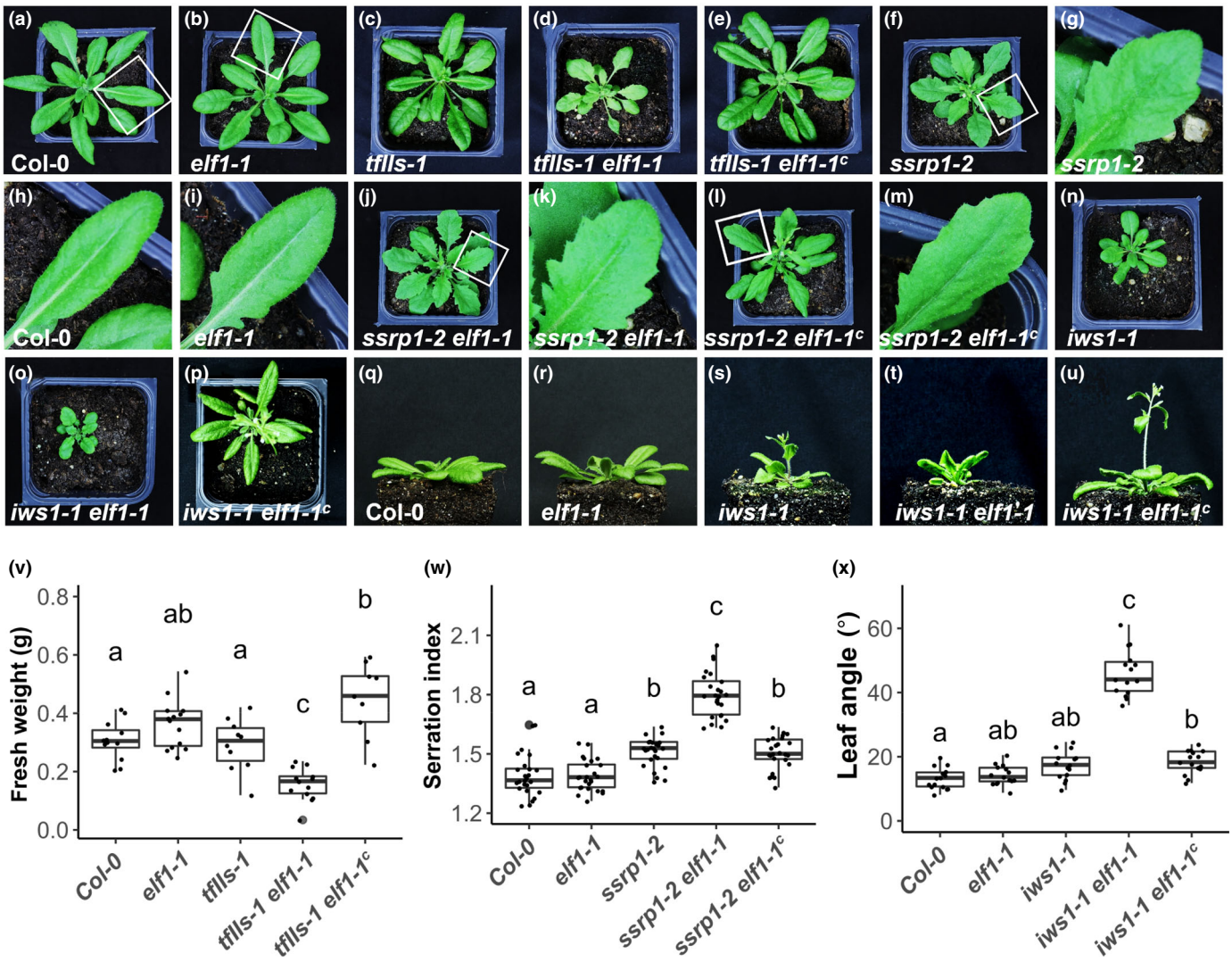

Fig. 5 In combination with other transcript elongation factor mutations, *elf1-1* leads to specific phenotypes that can be complemented by *pELF1::ELF1-eGFP*. (a–u) documentation of representative individuals illustrating overall and specific phenotypes of the indicated genotypes (Col-0, single- and double mutants, as well as complemented double mutants indicated by (c)). Compared with the parental lines, *tflls-1 elf1-1* exhibits a striking growth defect (d) and (v), while *ssrp1-2 elf1-1* is characterised by a prominent serrated leaf phenotype (j) and (w). The leaf phenotype is illustrated by the overall view of the rosette in (a, b, f, j, l) and the boxed areas are magnified in (g–i, k, m). Relative to the parental lines, the *iws1-1 elf1-1* double mutant exhibits remarkably more erect leaves (lateral view) due to a greater leaf angle (t, x). (v–x) Phenotypical analyses are visualised by plotting the median in boxplots with hinges corresponding to the first and third quartile, whisker range is 1.5 inter-quartile range of the respective hinge, and outliers are represented by dots. The outcome of statistical analysis of the indicated phenotypes using one-way ANOVA followed by Tukey's multiple comparison test is indicated by letters. All pictures have been taken, and statistical analysis has been performed with 28-d after stratification (DAS) plants.

clearly distinct from the controls (Fig. S6). While the controls did not yield distinguishable enrichment in genomic coverage, ChIP with ELF1-eGFP exhibited markedly increased coverage over RNAPII transcribed regions, beginning at TSSs with a distinctive maximum around transcriptional end sites (TESs; Fig. 6a). The distribution pattern over the transcribed regions resembles the profile of elongating RNAPII (Hetzel *et al.*, 2016; Zhu *et al.*, 2018; Yu *et al.*, 2019; Antosz *et al.*, 2020), and therefore, the ChIP coverage of ELF1-eGFP was compared with that determined for RNAPII-S2P (Fig. S7a). Both ELF1-eGFP and RNAPII-S2P are enriched over the transcribed regions of highly transcribed genes (based on RNA-Seq data) with a distinctive peak around the TES, but only background levels are detected over nontranscribed genes (Fig. 6b). Dividing the genes into four groups depending on transcript levels demonstrated that RNAPII-S2P and ELF1-eGFP coverage increases with higher transcript levels (Fig. S7b), illustrating the correlation of ELF1 occupancy with ongoing RNAPII transcription that is typical of elongation factors. Interestingly, of the protein-coding genes with a peak for RNAPII-S2P enrichment (n = 9969) only *c.* 33% (n = 3253) of these genes show also a peak for ELF1-eGFP enrichment (Fig. 6c).

This is also apparent at the level of individual genes, when comparing the distribution of the ChIP signals of ELF1-eGFP and RNAPII-S2P along with the corresponding transcript levels and controls (Fig. 6d). Here, next to transcribed loci with clear

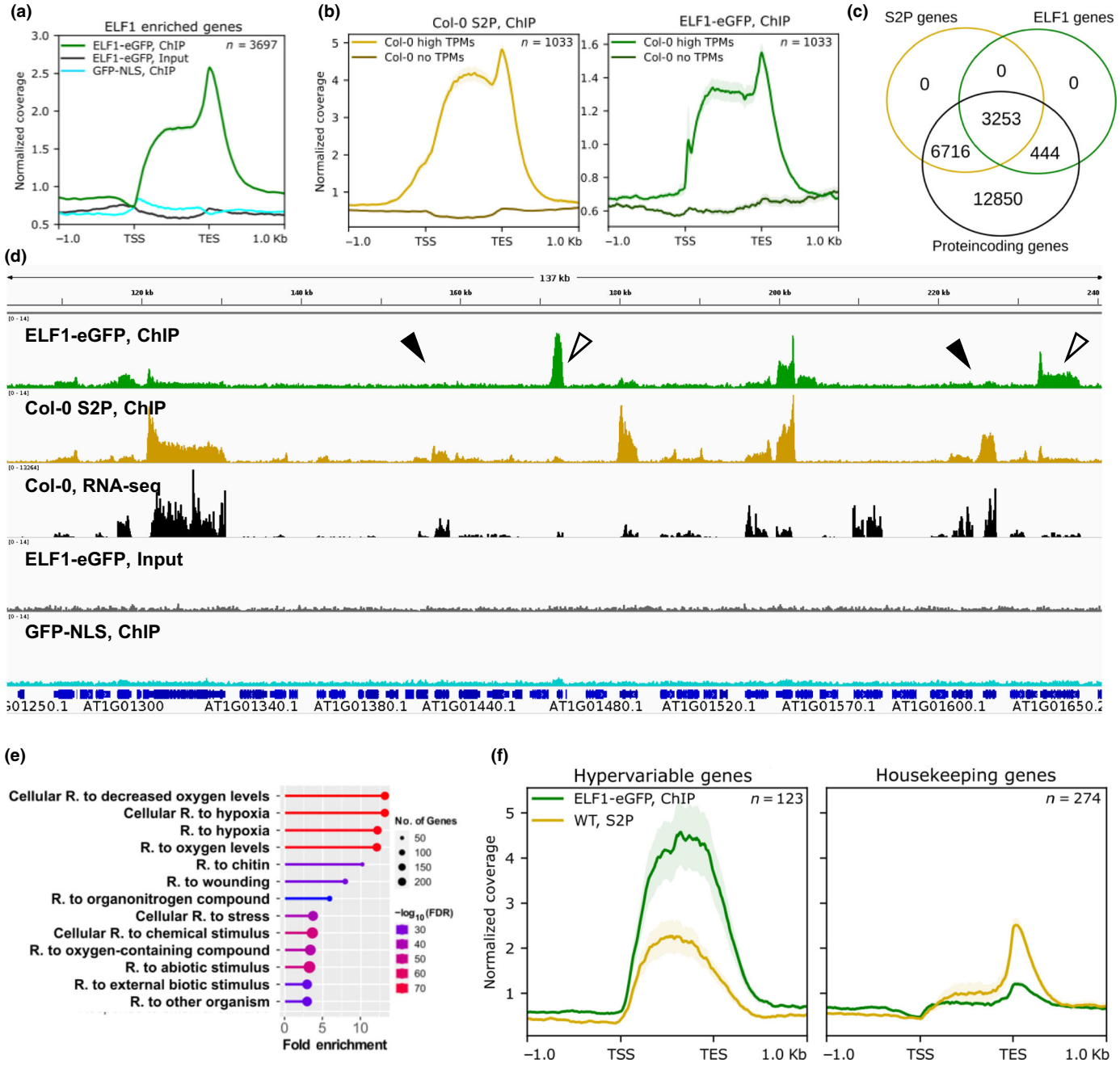

Fig. 6 ELF1 is enriched over transcribed regions of a subset of RNAPII transcribed genes. (a) Metagene analysis of ChIP sequencing (ChIP-Seq) data obtained using α-GFP-specific antibodies with *elf1-1*^{C} plants (expressing ELF1-eGFP) and control plants (expressing GFP-NLS) as well as *elf1-1*^{C} input samples. (b) ELF1-GFP and RNAPII-S2P chromatin immunoprecipitation (ChIP) signals were plotted over highly transcribed genes (> 28 TPM, based on RNA-Seq analysis) and nontranscribed genes (< 0.01 TPM). Mean signals of the biological replicates were averaged (line) and the tracks represent the SEM for the replicates at each position (shaded area). (c) Number of genes with ELF1-GFP occupancy relative to the number of genes with RNAPII-S2P coverage and the total number of protein-coding genes. (d) ChIP-Seq profiles of individual genes aligned with RNA-Seq data and controls, illustrating that some transcribed loci exhibit RNAPII-S2P coverage, but no ELF1-GFP enrichment (indicated by closed arrowheads), whereas at other loci, there is a particularly strong ELF1-GFP signal relative to the RNAPII-S2P coverage (indicated by open arrowheads). Gene models are shown at the bottom. (e) Gene Ontology (GO)-term analysis of genes showing the highest ELF1-GFP coverage relative to RNAPII-S2P coverage (n = 1000). Gene Ontology terms were sorted as indicated according to fold enrichment and number of genes per class with 'R.' representing 'response'. (f) ELF1-GFP and RNAPII-S2P ChIP signals were plotted over hypervariable and housekeeping genes (according to Zilberman *et al*., 2007; Aceituno *et al*., 2008).

RNAPII-S2P and ELF1-eGFP coverage, there are transcribed loci with RNAPII-S2P coverage, but without detectable ELF1-eGFP association (indicated by closed arrowheads). In addition, at few other loci there are – relative to the RNAPII-S2P coverage – remarkably prominent ELF1-GFP signals (indicated by open arrowheads). Loci with high ELF1-eGFP coverage are also apparent from unsupervised k-means clustering analysis (Fig. S8a). Gene Ontology analysis of genes showing the highest ELF1-

eGFP coverage demonstrated a clear enrichment for gene classes that are responsive to various stimuli (Fig. 6e). We further explored that by comparatively analysing the association of ELF1-eGFP with hypervariable relative to housekeeping genes (Zilberman *et al.*, 2007; Aceituno *et al.*, 2008). While 34 out of 123 hypervariable genes are highly enriched in ELF1-eGFP, only five out of 274 housekeeping genes exhibit prominent ELF1-eGFP coverage (Fig. S8b). This difference in ELF1-eGFP coverage is also evident from plotting the ChIP signals over these two gene classes (Fig. 6f). We extended this analysis by extracting genes of the GO terms 'responsive to stimulus' from TAIR10 (https://www.arabidopsis.org/). The ChIP signals of RNAPII-S2P and ELF1-eGFP colocalise over those genes as well as genes of the subgroups that are responsive to abiotic and biotic stimuli (Fig. S9). Interestingly, relative to the RNAPII-S2P signal, the ELF1-eGFP signal is particularly enriched on genes responsive to biotic stimuli. Sequence motif analysis using HOMER (Heinz *et al.*, 2010) of the 797 genes with high ELF1-eGFP coverage (cf. Fig. S8) revealed consistent results, as motifs including those of WRKY and AP2/ERF factors indicative of biotic and abiotic stress-responsive genes (Phukan *et al.*, 2016; Xie *et al.*, 2019) were clearly enriched (Fig. S10). Taken together, ELF1 associates over regions actively transcribed by RNAPII, which represents a characteristic feature of TEFs (Sims *et al.*, 2004; Kwak & Lis, 2013; van Lijsebettens & Grasser, 2014). Beyond that, ELF1 occupancy is detected over a subset of transcribed loci with a preference for inducible rather than for constitutively expressed genes.

Discussion

Besides SPT4-SPT5 and TFIIS, ELF1 is considered a 'basal' TEF that is conserved not only in eukaryotes, but also in archaea (Ehara & Sekine, 2018). Sequences with similarity to yeast ELF1 (and mammalian ELOF1) are encoded in plant genomes and in this work, we provide evidence that *Arabidopsis* ELF1 plays a role in transcript elongation by RNAPII. Apart from its amino acid sequence conservation compared with the orthologues from yeast and metazoa, ELF1 localises to nuclei in *Arabidopsis* cells. It prominently copurifies with RNAPII and various TEFs including SPT4-SPT5, SPT6L, IWS1, PAF1C and FACT, in line with results obtained with ELF1 proteins of other organisms (Ehara *et al.*, 2017, 2019; van der Weegen *et al.*, 2021). Moreover, characteristic for elongation factors ChIP experiments demonstrated that ELF1 specifically associates with the transcribed region of genes actively transcribed by RNAPII, resembling the distribution of *Arabidopsis* RNAPII-S2P and that of ELF1 in yeast (Mayer *et al.*, 2010; Rossi *et al.*, 2021). Finally, *ELF1* exhibits genetic interactions with genes encoding other *Arabidopsis* elongation factors such as TFIIS, SSRP1 and IWS1. Yeast *ELF1* genetically interacted with *TFIIS* and genes encoding additional TEFs such as SPT4-SPT5, SPT6, SPT16 and PAF1C (Prather *et al.*, 2005), while human *ELOF1* showed interaction with *SPT4-SPT5, SPT6, CTR9* and *LEO1* (van der Weegen *et al.*, 2021).

In agreement with the yeast *elf1Δ* mutation that caused no significant growth defect (Prather *et al.*, 2005), *Arabidopsis elf1-1* exhibits basically wild-type appearance. A rice mutant defective in a possible *ELF1* orthologue termed *OsTEF1* showed reduced tillering capacity and retarded growth of seminal roots (Paul *et al.*, 2012), while inactivation of a putative wheat orthologue termed *TaTEF-7A* modulates grain number per spike (Zheng *et al.*, 2014). The observation that the *elf1-1* mutation does not cause significant growth defects, resembles the situation with *tfIIs* mutant plants that also grow similar to wild-type under standard conditions (Grasser *et al.*, 2009), but exhibit a striking sensitivity when exposed to elevated temperatures (Szádeczky-Kardoss *et al.*, 2022). Moreover, *Arabidopsis* plants defective in PAF1C subunits display reduced tolerance to increased salt concentrations and are affected in the response to mechanical stimulation (Jensen *et al.*, 2017; Obermeyer *et al.*, 2022; Zhang *et al.*, 2022). Likewise, expression of ELF1 may prove relevant under certain environmental conditions, since ELF1 associates preferentially with genes that are responsive to biotic and abiotic stress responses. Combination of the *elf1-1* mutation with genes encoding other *Arabidopsis* TEFs resulted in distinct phenotypic alterations. Thus, despite the wild-type appearance of the parental lines the *elf1-1 tfIIs-1* double mutant exhibits markedly reduced growth. However, the *elf1-1 ssrp1-2* plants are characterised by prominent leaf serration, while *elf1-1 iws1-1* plants are sterile and display strikingly altered leaf inclination resulting in more vertically oriented leaves. The phenotypes observed with the various double-mutant combinations suggest that the interaction of ELF1 with other TEFs may result in (partially) different transcriptional output in *Arabidopsis*.

Because of its constant association with the elongation complex during transcription, yeast ELF1 is designated as core elongation factor (Joo *et al.*, 2019), and likewise, archaeal ELF1 is a general part of the elongation complex (Blombach *et al.*, 2021). Based on our ChIP-Seq analyses, *Arabidopsis* ELF1 associates only with *c.* 33% of the RNAPII transcribed loci. Interestingly, ELF1 is detected preferentially along inducible genes rather than at constitutively expressed genes. Generally, the relative magnitude of the ELF1 and RNAPII-S2P ChIP-Seq signals appears to vary considerably, which may suggest that some genes require a greater amount of ELF1 for proper transcription, while other genes can be efficiently transcribed in the absence of ELF1. In addition to increased sensitivity of current mass spectrometry and the small size of the ELF1 protein, its association with only a subpopulation of RNAPII elongation complexes could account for the fact that ELF1 was not detected in previous mass spectrometric analyses of the *Arabidopsis* RNAPII elongation complex (Antosz *et al.*, 2017).

Recent *in vitro* transcription experiments on reconstituted nucleosomal templates and structural cryo-EM analyses indicated that *Komagataella pastoris* ELF1 promotes nucleosome transcription by RNAPII. Particularly, in combination with SPT4-SPT5, ELF1 exhibited a strong synergistic effect on RNAPII progression on the nucleosome (Ehara *et al.*, 2019). ELF1 and SPT4-SPT5 together reshape the downstream edge of the RNAPII elongation complex. In this scenario, the conserved basic N-terminal region of ELF1 could interact with the nucleosomal DNA, assisting dissociation of histone–DNA contacts, which is favourable for

RNAPII progression through nucleosomes (Ehara *et al.*, 2019). Our *in vitro* interaction studies demonstrated that *Arabidopsis* ELF1 binds to histones via its C-terminal acidic region, while the N-terminal basic region proved relevant for DNA interactions. Individual ELF1 appears to exist in an autoinhibited conformation, in which the acidic C-terminal region can be crosslinked intramolecularly with basic parts of the protein. This reminds of chromosomal HMGB proteins, whose acidic C-terminal region interacts with the basic DNA-binding parts of the protein to modulate DNA interactions (Thomsen *et al.*, 2004; Stott *et al.*, 2014). In case of *Arabidopsis* ELF1, during chromatin transcription by RNAPII, the acidic C-terminal region could interact with nucleosomal histones, at the same time releasing the basic N-terminal region from autoinhibition to interact with the DNA of the approached nucleosome, facilitating separation of histone–DNA contacts. According to a current model (Kujirai & Kurumizaka, 2020), ELF1 may contribute to the multiple acidic regions occurring in various TEFs including ELF1, SPT4-SPT5, PAF1C, FACT and SPT6 that in the RNAPII elongation complex may bind basic regions of the nucleosome exposed by the remodelling process during ongoing transcription.

Our study has revealed that ELF1 is a component of the RNAPII elongation complex in plants. Its role in transcriptional elongation is also evident from genetic interactions of *ELF1* with genes encoding other TEFs such as TFIIS, SSRP1 and IWS1, as well as its association with the transcribed region of active genes. ELF1 is enriched particularly along inducible RNAPII transcribed genes, basically sharing the genomic distribution with elongating RNAPII. The molecular analyses presented here provide a valuable resource and may inspire future studies addressing the contribution of transcriptional elongation to adjusting plant gene expression programmes under diverse conditions.

Acknowledgements

We thank Serena Herzinger and Emilia Polz for contributions to the project, Eduard Hochmuth for recording mass spectra, the Genomics Core Facility at the University of Regensburg (http://www.kfb-regensburg.de/) for high-throughput sequencing and the Nottingham Arabidopsis Stock Centre (NASC) for providing *Arabidopsis* T-DNA insertion lines. This research was supported by the German Research Foundation (DFG) through grants Gr1159/14-2 and SFB960/A6 to KDG. Open Access funding enabled and organized by Projekt DEAL.

Competing interests

None declared.

Author contributions

GL, FB and KDG designed the research and supervised the project. HM, PM-H, SO, CT, SB and AO performed experiments. HM, PM-H, SO, SB, AB and AO analysed data. KDG wrote the manuscript. All authors discussed the results, commented the manuscript and approved the final version.

ORCID

Klaus D. Grasser https://orcid.org/0000-0002-7080-5520

Data availability

Sequencing data have been deposited to the NCBI sequence read archive with the accession nos.: ChIP-Seq data of ELF1-eGFP and GFP-NLS (accession no. PRJNA823592), ChIP-Seq data of RNAPII-S2P (accession no. PRJNA826267) and RNA-Seq 6-DAS Col-0 (accession no. PRJNA758800).

References

Aceituno FF, Moseyko N, Rhee SY, Gutiérrez RA. 2008. The rules of gene expression in plants: organ identity and gene body methylation are key factors for regulation of gene expression in *Arabidopsis thaliana*. *BMC Genomics* **9**: 438.

Antosz W, Deforges J, Begcy K, Bruckmann A, Poirier Y, Dresselhaus T, Grasser KD. 2020. Critical role of transcript cleavage in Arabidopsis RNA polymerase II transcriptional elongation. *Plant Cell* **32**: 1449–1463.

Antosz W, Pfab A, Ehrnsberger HF, Holzinger P, Köllen K, Mortensen SA, Bruckmann A, Schubert T, Längst G, Griesenbeck J *et al.* 2017. The composition of the Arabidopsis RNA polymerase II transcript elongation complex reveals the interplay between elongation and mRNA processing factors. *Plant Cell* **29**: 854–870.

Berr A, McCallum EJ, Ménard R, Meyer D, Fuchs J, Dong A, Shen W-H. 2010. Arabidopsis SET DOMAIN GROUP2 is required for H3K4 trimethylation and is crucial for both sporophyte and gametophyte development. *Plant Cell* **22**: 3232–3248.

Bilsborough GD, Runions A, Barkoulas M, Jenkins HW, Hasson A, Galinha C, Laufs P, Hay A, Prusinkiewicz P, Tsiantis M. 2011. Model for the regulation of *Arabidopsis thaliana* leaf margin development. *Proceedings of the National Academy of Sciences, USA* **108**: 3424–3429.

Blombach F, Fouqueau T, Matelska D, Smollett K, Werner F. 2021. Promoter-proximal elongation regulates transcription in archaea. *Nature Communications* **12**: 5524.

Chen C, Shu J, Li C, Thapa RK, Nguyen V, Yu K, Yuan Z-C, Kohalmi SE, Liu J, Marsolais F *et al.* 2019. RNA polymerase II-independent recruitment of SPT6L at transcription start sites in Arabidopsis. *Nucleic Acids Research* **47**: 6714–6725.

Chen FX, Smith ER, Shilatifard A. 2018. Born to run: control of transcription elongation by RNA polymerase II. *Nature Reviews. Molecular Cell Biology* **19**: 464–478.

Cheng J, Xu L, Bergér V, Bruckmann A, Yang C, Schubert V, Grasser KD, Schnittger A, Zheng B, Jiang H. 2022. H3K9 demethylases IBM1 and JMJ27 are required for male meiosis in *Arabidopsis thaliana*. *New Phytologist* **235**: 2252–2269.

Dürr J, Lolas IB, Sørensen BB, Schubert V, Houben A, Melzer M, Deutzmann R, Grasser M, Grasser KD. 2014. The transcript elongation factor SPT4/SPT5 is involved in auxin-related gene expression in Arabidopsis. *Nucleic Acids Research* **42**: 4332–4347.

Ehara H, Kujirai T, Fujino Y, Shirouzu M, Kurumizaka H, Sekine S-I. 2019. Structural insight into nucleosome transcription by RNA polymerase II with elongation factors. *Science* **363**: 744–747.

Ehara H, Sekine S-I. 2018. Architecture of the RNA polymerase II elongation complex: new insights into Spt4/5 and Elf1. *Transcription* **9**: 286–291.

Ehara H, Yokoyama T, Shigematsu H, Yokoyama S, Shirouzu M, Sekine SI. 2017. Structure of the complete elongation complex of RNA polymerase II with basal factors. *Science* **357**: 921–924.

Ewels P, Magnusson M, Lundin S, Käller M. 2016. MultiQC: summarize analysis results for multiple tools and samples in a single report. *Bioinformatics* **32**: 3047–3048.

Fiorucci A-S, Bourbousse C, Concia L, Rougée M, Deton-Cabanillas A-F, Zabulon G, Layat E, Latrasse D, Kim SK, Chaumont N *et al.* 2019.

Arabidopsis S2Lb links AtCOMPASS-like and SDG2 activity in H3K4me3 independently from histone H2B monoubiquitination. *Genome Biology* **20**: 100.

Fleury D, Himanen K, Cnops G, Nelissen H, Boccardi TM, Maere S, Beemster GTS, Neyt P, Anami S, Robles P *et al.* 2007. The *Arabidopsis thaliana* homolog of yeast BRE1 has a function in cell cycle regulation during early leaf and root growth. *Plant Cell* **19**: 417–432.

Ge SX, Jung D, Yao R. 2020. ShinyGO: a graphical gene-set enrichment tool for animals and plants. *Bioinformatics* **36**: 2628–2629.

Grasser KD, Grimm R, Ritt C. 1996. Maize chromosomal HMGc: two closely related structure-specific DNA-binding proteins specify a second type of plant HMG-box protein. *The Journal of Biological Chemistry* **271**: 32900–32906.

Grasser M, Kane CM, Merkle T, Melzer M, Emmersen J, Grasser KD. 2009. Transcript elongation factor TFIIS is involved in *Arabidopsis* seed dormancy. *Journal of Molecular Biology* **386**: 598–611.

Gu XL, Wang H, Huang H, Cui XF. 2012. SPT6L encoding a putative WG/GW-repeat protein regulates apical-basal polarity of embryo in *Arabidopsis*. *Molecular Plant* **5**: 249–259.

He Y, Doyle MR, Amasino RM. 2004. PAF1-complex-mediated histone methylation of *FLOWERING LOCUS C* chromatin is required for the vernalization-responsive, winter-annual habit in *Arabidopsis*. *Genes & Development* **18**: 2774–2784.

Heinz S, Benner C, Spann N, Bertolino E, Lin YC, Laslo P, Cheng JX, Murre C, Singh H, Glass CK. 2010. Simple combinations of lineage-determining transcription factors prime cis-regulatory elements required for macrophage and B cell identities. *Molecular Cell* **38**: 576–589.

Hetzel J, Duttke SH, Benner C, Chory J. 2016. Nascent RNA sequencing reveals distinct features in plant transcription. *Proceedings of the National Academy of Sciences, USA* **113**: 12316–12321.

Hopkins R, Schmitt J, Stinchcombe JR. 2008. A latitudinal cline and response to vernalization in leaf angle and morphology in *Arabidopsis thaliana* (Brassicaceae). *New Phytologist* **179**: 155–164.

Jensen GS, Fal K, Hamant O, Haswell ES. 2017. The RNA polymerase-associated factor 1 complex is required for plant touch responses. *Journal of Experimental Botany* **68**: 499–511.

Joo YJ, Ficarro SB, Chun Y, Marto JA, Buratowski S. 2019. *In vitro* analysis of RNA polymerase II elongation complex dynamics. *Genes & Development* **33**: 578–589.

Kujirai T, Kurumizaka H. 2020. Transcription through the nucleosome. *Current Opinion in Structural Biology* **61**: 42–49.

Kwak H, Lis JT. 2013. Control of transcriptional elongation. *Annual Review of Genetics* **47**: 483–508.

Langmead B, Salzberg SL. 2012. Fast gapped-read alignment with Bowtie 2. *Nature Methods* **9**: 357–359.

van Leene J, Eeckhout D, Cannoot B, De Winne N, Persiau G, Van De Slijke E, Vercruysse L, Dedecker M, Verkest A, Vandepoele K *et al.* 2015. An improved toolbox to unravel the plant cellular machinery by tandem affinity purification of *Arabidopsis* protein complexes. *Nature protocols* **10**: 169–187.

Li L, Ye H, Guo H, Yin Y. 2010. *Arabidopsis* IWS1 interacts with transcription factor BES1 and is involved in plant steroid hormone brassinosteroid regulated gene expression. *Proceedings of the National Academy of Sciences, USA* **107**: 3918–3923.

van Lijsebettens M, Grasser KD. 2014. Transcript elongation factors: shaping transcriptomes after transcript initiation. *Trends in Plant Science* **19**: 717–726.

Liu H, Ding Y, Zhou Y, Jin W, Xie K, Chen L-L. 2017. CRISPR-P 2.0: an improved CRISPR-Cas9 tool for genome editing in plants. *Molecular Plant* **10**: 530–532.

Lolas IB, Himanen K, Grønlund JT, Lynggaard C, Houben A, Melzer M, van Lijsebettens M, Grasser KD. 2010. The transcript elongation factor FACT affects Arabidopsis vegetative and reproductive development and genetically interacts with HUB1/2. *The Plant Journal* **61**: 686–697.

Mayer A, Lidschreiber M, Siebert M, Leike K, Söding J, Cramer P. 2010. Uniform transitions of the general RNA polymerase II transcription complex. *Nature Structural & Molecular Biology* **17**: 1272–1278.

Michl-Holzinger P, Obermeyer S, Markusch H, Pfab A, Ettner A, Bruckmann A, Babl S, Längst G, Schwartz U, Tvardovskiy A *et al.* 2022. Phosphorylation of the FACT histone chaperone subunit SPT16 affects chromatin at RNA polymerase II transcriptional start sites in *Arabidopsis*. *Nucleic Acids Research* **50**: 5014–5028.

Municio C, Antosz W, Grasser KD, Kornobis E, van Bel M, Eguinoa I, Coppens F, Bräutigam A, Lermontova I, Bruckmann A *et al.* 2021. The Arabidopsis condensin CAP-D subunits arrange interphase chromatin. *New Phytologist* **230**: 972–987.

Obermeyer S, Stöckl R, Schnekenburger T, Moehle C, Schwartz U, Grasser KD. 2022. Distinct role of subunits of the Arabidopsis RNA polymerase II elongation factor PAF1C in transcriptional reprogramming. *Frontiers in Plant Science* **13**: 974625.

Oh S, Zhang H, Ludwig P, van Nocker S. 2004. A mechanism related to the yeast transcriptional regulator Paf1c is required for expression of the *Arabidopsis FLC/MAF* MADS box gene family. *Plant Cell* **16**: 2940–2953.

Osakabe A, Lorkovic ZJ, Kobayashi W, Tachiwana H, Yelagandula R, Kurumizaka H, Berger F. 2018. Histone H2A variants confer specific properties to nucleosomes and impact on chromatin accessibility. *Nucleic Acids Research* **46**: 7675–7685.

Osman S, Cramer P. 2020. Structural biology of RNA polymerase II transcription: 20 years on. *Annual Review of Cell and Developmental Biology* **36**: 1–34.

Paul P, Awasthi A, Rai AK, Gupta SK, Prasad R, Sharma TR, Dhaliwal HS. 2012. Reduced tillering in Basmati rice T-DNA insertional mutant OsTEF1 associates with differential expression of stress related genes and transcription factors. *Functional & Integrative Genomics* **12**: 291–304.

Pfab A, Grønlund JT, Holzinger P, Längst G, Grasser KD. 2018. The Arabidopsis histone chaperone FACT: role of the HMG-box domain of SSRP1. *Journal of Molecular Biology* **430**: 2747–2759.

Phukan UJ, Jeena GS, Shukla RK. 2016. WRKY transcription factors: molecular regulation and stress responses in plants. *Frontiers in Plant Science* **7**: 760.

Prather D, Krogan NJ, Emili A, Greenblatt JF, Winston F. 2005. Identification and characterization of Elf1, a conserved transcription elongation factor in *Saccharomyces cerevisiae*. *Journal of Molecular Cell Biology* **25**: 10122–10135.

Quadrana L, Bortolini Silveira A, Mayhew GF, LeBlanc C, Martienssen RA, Jeddeloh JA, Colot V. 2016. The *Arabidopsis thaliana* mobilome and its impact at the species level. *eLife* **5**: e15716.

Ramírez F, Ryan DP, Grüning B, Bhardwaj V, Kilpert F, Richter AS, Heyne S, Dündar F, Manke T. 2016. deepTools2: a next generation web server for deep-sequencing data analysis. *Nucleic Acids Research* **44**: W160–W165.

Rossi MJ, Kuntala PK, Lai WKM, Yamada N, Badjatia N, Mittal C, Kuzu G, Bocklund K, Farrell NP, Blanda TR *et al.* 2021. A high-resolution protein architecture of the budding yeast genome. *Nature* **592**: 309–314.

Sims RJ, Belotserkovskaya R, Reinberg D. 2004. Elongation by RNA polymerase II: the short and long of it. *Genes & Development* **18**: 2437–2468.

Stott K, Watson M, Bostock MJ, Mortensen SA, Travers A, Grasser KD, Thomas JO. 2014. Structural insights into the mechanism of negative regulation of single-box high mobility group proteins by the acidic tail domain. *The Journal of Biological Chemistry* **289**: 29817–29826.

Szádeczky-Kardoss I, Szaker HM, Verma R, Darkó É, Pettkó-Szandtner A, Silhavy D, Csorba T. 2022. Elongation factor TFIIS is essential for heat stress adaptation in plants. *Nucleic Acids Research* **50**: 1927–1950.

Thomsen MS, Franssen L, Launholt D, Fojan P, Grasser KD. 2004. Interactions of the basic N-terminal and the acidic C-terminal domains of the maize chromosomal HMGB1 protein. *Biochemistry* **43**: 8029–8037.

Wang Z-P, Xing H-L, Dong L, Zhang H-Y, Han C-Y, Wang X-C, Chen Q-J. 2015. Egg cell-specific promoter-controlled CRISPR/Cas9 efficiently generates homozygous mutants for multiple target genes in Arabidopsis in a single generation. *Genome Biology* **16**: 144.

van der Weegen Y, de Lint K, van den Heuvel D, Nakazawa Y, Mevissen TET, van Schie JJM, San Martin Alonso M, Boer DEC, González-Prieto R, Narayanan IV *et al.* 2021. ELOF1 is a transcription-coupled DNA repair factor that directs RNA polymerase II ubiquitylation. *Nature Cell Biology* **23**: 595–607.

Winter D, Vinegar B, Nahal H, Ammar R, Wilson GV, Provart NJ. 2007. An "electronic fluorescent pictograph" browser for exploring and analyzing large-scale biological data sets. *PLoS ONE* **2**: e718.

Xie Z, Nolan TM, Jiang H, Yin Y. 2019. AP2/ERF transcription factor regulatory networks in hormone and abiotic stress responses in Arabidopsis. *Frontiers in Plant Science* **10**: 228.

Xu L, Zhao Z, Dong A, Soubigou-Taconnat L, Renou JP, Steinmetz A, Shen W-H. 2008. Di- and tri- but not monomethylation on histone H3 lysine 36 marks active transcription of genes involved in flowering time regulation and other processes in *Arabidopsis thaliana*. *Journal of Molecular Cell Biology* **28**: 1348–1360.

Yu X, Martin PGP, Michaels SD. 2019. BORDER proteins protect expression of neighboring genes by promoting 3′ Pol II pausing in plants. *Nature Communications* **10**: 4359.

Zhang H, Li X, Song R, Zhan Z, Zhao F, Li Z, Jiang D. 2022. Cap-binding complex assists RNA polymerase II transcription in plant salt stress response. *Plant, Cell & Environment* **45**: 2780–2793.

Zheng J, Liu H, Wang Y, Wang L, Chang X, Jing R, Hao C, Zhang X. 2014. TEF-7A, a transcript elongation factor gene, influences yield-related traits in bread wheat (*Triticum aestivum* L.). *Journal of Experimental Botany* **65**: 5351–5365.

Zhu J, Liu M, Liu X, Dong Z. 2018. RNA polymerase II activity revealed by GRO-seq and pNET-seq in *Arabidopsis*. *Nature Plants* **4**: 1112–1123.

Zilberman D, Gehring M, Tran RK, Ballinger T, Henikoff S. 2007. Genome-wide analysis of *Arabidopsis thaliana* DNA methylation uncovers an interdependence between methylation and transcription. *Nature Genetics* **39**: 61–69.

Zlatanova J, van Holde K. 1998. Binding to four-way junction DNA: a common property of architectural proteins? *The FASEB Journal* **12**: 421–431.

Supporting Information

Additional Supporting Information may be found online in the Supporting Information section at the end of the article.

Fig. S1 Amino acid sequence alignment of ELF1 of different species.

Fig. S2 Generation of the *elf1-1* gene editing mutant and *elf1-1 pELF1::ELF1-eGFP* complementation line.

Fig. S3 Phenotype of *tfIIs elf1* double-mutant plants.

Fig. S4 Phenotype of *ssrp1 elf1* double-mutant plants.

Fig. S5 Phenotype of *iws1 elf1* double-mutant plants.

Fig. S6 Chromatin immunoprecipitation sequencing replicates show high pairwise correlation.

Fig. S7 Comparative coverage profiles of ELF1-eGFP and RNA polymerase II-S2P.

Fig. S8 Differential coverage of genes with ELF1.

Fig. S9 ELF1-eGFP and RNAPII-S2P coverage over genes responsive to stimuli.

Fig. S10 Motif analysis of ELF1-enriched genes.

Table S1 Plasmids used in this study.

Table S2 Oligonucleotides used in this study.

Table S3 Summary of chromatin immunoprecipitation sequencing statistics for this project.

Please note: Wiley is not responsible for the content or functionality of any Supporting Information supplied by the authors. Any queries (other than missing material) should be directed to the *New Phytologist* Central Office.